Direct measurement of the evanescent-wave polarization state

Leszek Józefowski, Jacek Fiutowski, and Tomasz Kawalec

Marian Smoluchowski Institute of Physics, Jagiellonian University, Ul. Reymonta 4, 30-059 Krakow, Poland

Horst-Günter Rubahn

Mads Clausen Institute, University of Southern Denmark, Dybbolsgaa 2—Alsion, DK-6400 Sonderborg, Denmark

Received June 1, 2006; accepted October 14, 2006;
posted October 31, 2006 (Doc. ID 71610); published February 15, 2007

We present results from a direct measurement of the elliptical character of the evanescent part of linearly in-plane polarized light, totally internally reflected from a quartz half-sphere. These results have been obtained by invoking polarization-sensitive and light-emitting organic nanofibers. The angular dependencies of the mean-square electric field vector components parallel and perpendicular to the surface plane agree with predictions from the Fresnel equations. © 2007 Optical Society of America

OCIS codes: 260.6970, 260.5430, 160.4640.

INTRODUCTION

Polarization properties of electromagnetic waves become particularly important when we consider propagation in media with boundary conditions. Examples include optical fibers and planar waveguides or simply the interface-connecting media with different refractive indices. Even in the case of isotropic media a scalar approach to light wave scattering is not sufficient, and the polarization of the waves plays an important role. Let us consider total internal reflection (TIR), a phenomenon that is underlying the important domain of guided waves and is thus crucial for optical information transmission and processing. In contrast to common plane waves propagating in extended media, the planes of constant phase and constant amplitude are not parallel for the evanescent wave (EW). This property of the EW (called inhomogeneity) is connected to the nontransversality of electric or magnetic components of the electromagnetic field. In this article we present systematic optical investigations of this phenomenon, employing a new kind of polarized light emitting and absorbing nanoaggregates, namely, organic crystalline nanofibers.

Note that the polarization behavior and features of the EW are rarely considered in details in the optics literature.[1,2] If the incident beam is linearly polarized in the plane perpendicular to the plane of incidence (TE polarization), then the polarization of the EW does not change upon reflection. If the incidence wave, however, is polarized in the plane of incidence (TM polarization), then the EW is predicted to be elliptically polarized.[3]

THEORY

Let us assume a monochromatic plane wave that reaches the border of two nonmagnetic media with an angle larger than the critical angle, as seen in Fig. 1.

For the considered planar border between two media for any case of polarization of the incident wave, it is sufficient to perform calculations and measurements for either TE or TM polarizations.

Mean-square values of the electric field vector components in the dilute medium for angles of θ in the range from 0 to 90 deg behave as[4]

$$\langle E_y^2 \rangle = \frac{1}{2}|t_{TE}|^2 e^{-4\pi z/\lambda \,\mathrm{Im}\,\sqrt{n_2^2 - n_1^2 \sin^2\theta}} E_{0TE}^2, \tag{1}$$

$$\langle E_x^2 \rangle = \frac{1}{2}\left|\frac{\sqrt{n_2^2 - n_1^2 \sin^2\theta}}{n_2} t_{TM}\right|^2 \times e^{-4\pi z/\lambda \,\mathrm{Im}\,\sqrt{n_2^2 - n_1^2 \sin^2\theta}} E_{0TM}^2, \tag{2}$$

$$\langle E_z^2 \rangle = \frac{1}{2}\left|\frac{n_1 \sin\theta}{n_2} t_{TM}\right|^2 e^{-4\pi z/\lambda \,\mathrm{Im}\,\sqrt{n_2^2 - n_1^2 \sin^2\theta}} E_{0TM}^2, \tag{3}$$

where the transmittance coefficients t_{TE} and t_{TM} are given as

$$t_{TE} = \frac{2n_1 \cos\theta}{n_1 \cos\theta + \sqrt{n_2^2 - n_1^2 \sin^2\theta}}, \tag{4}$$

$$t_{TM} = \frac{2n_1 n_2 \cos\theta}{n_2^2 \cos\theta + n_1\sqrt{n_2^2 - n_1^2 \sin^2\theta}}, \tag{5}$$

with λ the wavelength of the light.

With the help of Eqs. (1)–(3) we calculate mean-square values of the electric field at the border surface ($z = 0$) as a function of the angle of incidence (Fig. 2).

It is useful to calculate the EW electric field components in order to extract the information about phase relations between the components of the electric field vector[2,3]:

$$\frac{E_x}{E_{0TM}} = \frac{2\cos\theta\sqrt{\sin^2\theta - n_{21}^2}}{\sqrt{n_{21}^4\cos^2\theta + \sin^2\theta - n_{21}^2}} e^{(-i(\delta^{TM}+\pi)/2)}, \quad (6)$$

$$\frac{E_y}{E_{0TE}} = \frac{2\cos\theta}{\sqrt{1-n_{21}^2}} e^{(-i\delta^{TE}/2)}, \quad (7)$$

$$\frac{E_z}{E_{0TM}} = \frac{2\cos\theta\sin\theta}{\sqrt{n_{21}^4\cos^2\theta + \sin^2\theta - n_{21}^2}} e^{(-i\delta^{TM}/2)}, \quad (8)$$

where, $n_{21}=n_2/n_1$ and δ^{TM} and δ^{TE} are the phase shifts of appropriate polarization wave vectors when totally internally reflected.

It is obvious that in the TE polarization case that the EW is linearly polarized with its electric vector parallel to the border surface and perpendicular to the plane of incidence. In the TM polarization case there are two components above the critical angle, shifted in phase by $\pi/2$. This results in an elliptical polarization in the plane of incidence. Figure 3 summarizes this behavior.[3]

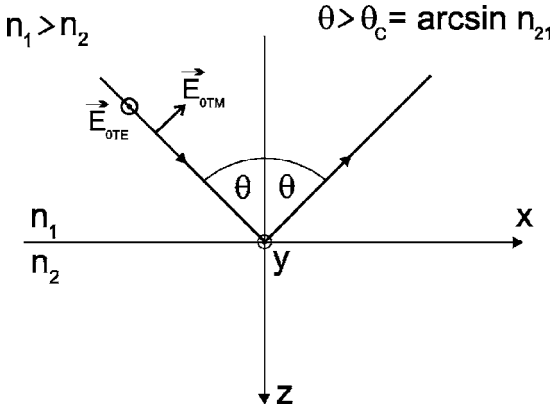

Fig. 1. Plane wave on the dielectric interface at TIR, showing the coordinate system and the definition of TE and TM polarization cases. E_{0TE} and E_{0TM} are electric vectors of the incident wave.

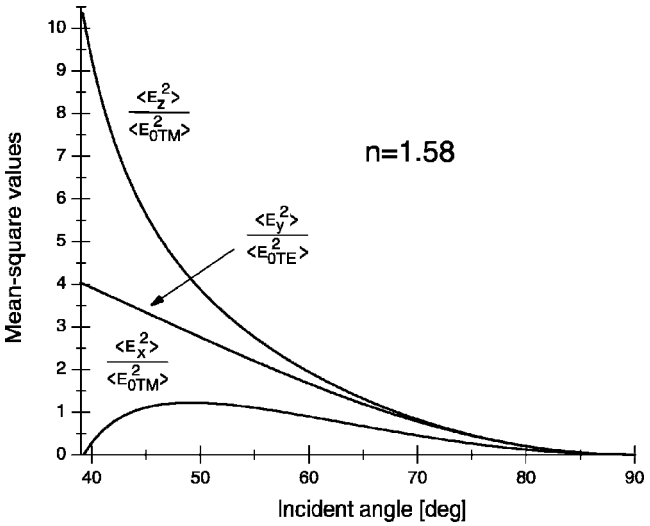

Fig. 2. Mean-square electric field components at the mica—air interface for $n_1=1.58$ and $n_2=1$ as a function of the angle of incidence.

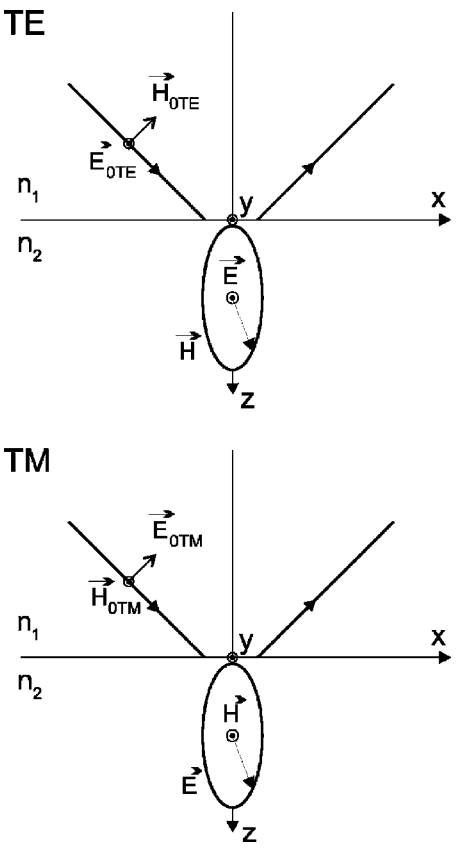

Fig. 3. Predicted state of polarization of EW for TE and TM polarizations of the incident wave.

To prove this prediction experimentally a polarization-sensitive phenomenon at the interface or surface has to be employed. This could be done for example by using an indirect spectroscopic method, such as the Zeeman effect in an atomic vapor. Thanks to an applied magnetic field, the Zeeman components for an atomic transition split. Different contributions of π and σ lines for magnetic fields parallel or perpendicular to the plane of incidence will then give a qualitative proof of the elliptical character of the EW in the TM case.[5] In the present experiment we quantitatively prove the elliptical character by using organic nanofibers or "needles" grown on a muscovite mica surface from parahexaphenylene (p6P) molecules.[6] Under special circumstances millimeter-sized domains of long, parallel-oriented needles are created, consisting of molecules that have their optical axes positioned nearly parallel to the mica surface, namely about 85 deg to the surface normal, and nearly perpendicular to the needles' axes.[7] Lengths of the nanofibers range to several hundred micrometers, widths are of the order of 400 nm, and heights are between a few tens and one hundred nanometers. Because of the small size, extremely high luminescence efficiencies, and large polarization ratios, the nanofibers are extraordinarily good probes of the EW. They absorb polarized light in the wavelength range between 320 and 360 nm and re-emit it centered between 420 and 450 nm.[6]

EXPERIMENTAL

The main idea of the experiment is to rotate a flat domain of parallel-oriented needles over an angle of 2π and to excite the domain with polarized UV EW radiation while detecting simultaneously the emitted fluorescence intensity. In TE polarization the result should be a sinusoidal intensity distribution with two maxima corresponding to the superposition of the projection of the optical axis of the needles' molecules on the *XY* plane with the direction of the electric vector of the EW. In fact, the distribution function should be identical with the volume-wave excitation case.[8] In the TM case if no ellipticity were present one should observe a flat fluorescence intensity curve when rotating the domain, since the molecules are laying nearly flat on the surface and thus their rotation is not changing their angle with respect to the incoming field vector. Any residual sinusoidal function would be due to the *x* component of the electric vector and would prove the elliptical character of the EW. If present, the sinusoidal TM curve should be shifted by $\pi/2$ with respect to the TE curve.

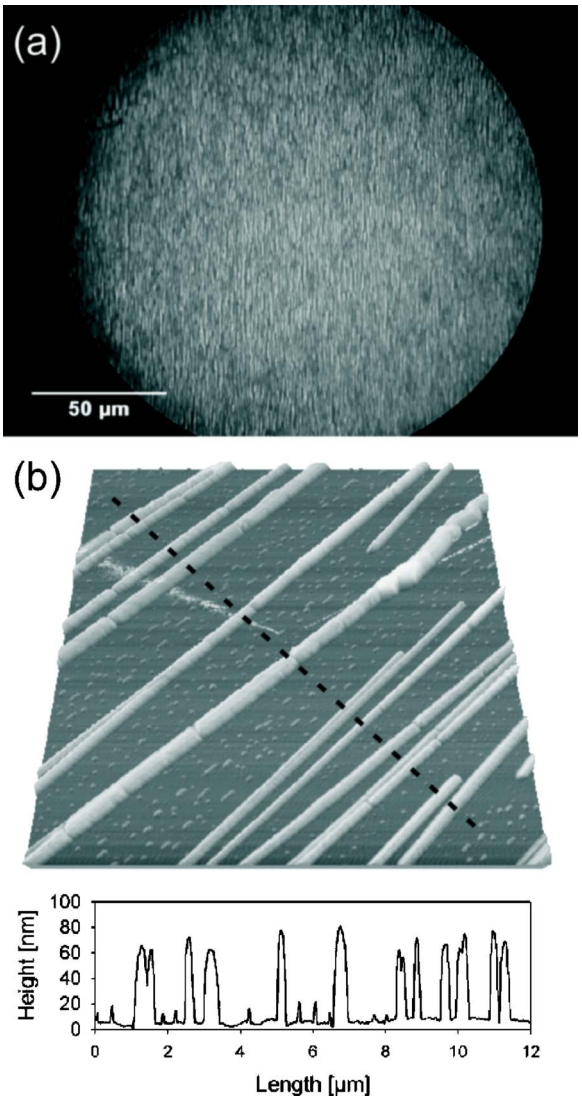

Fig. 4. (a) Fluorescence microscopy image (excitation at 370 nm) of a dense array of nanofibers. (b) Atomic force microscopy image (10×10 μm^2) of a similar dense array, denoting the uniform height. The dashed line represents the position of the cross section presented at the bottom.

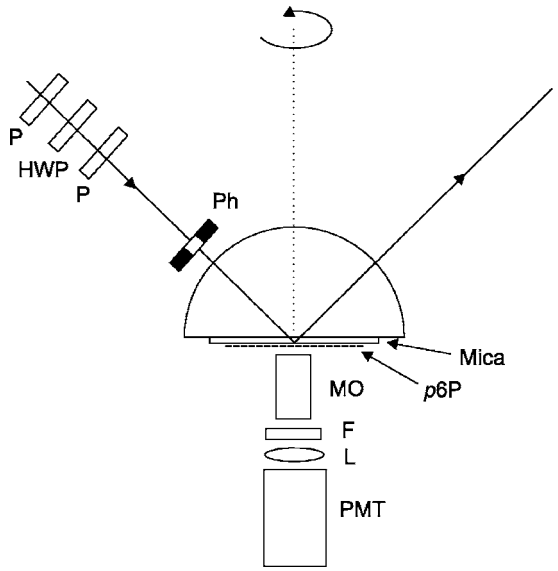

Fig. 5. Experimental setup. MO, microscope objective; F, filter; PMT, photomultiplier; Ph, pinhole; P, polarizer; HWP, half-wave plate.

To obtain EW excitation we have used a half-sphere made of fused silica $n=1.48$ at 325 nm with a radius of 10 mm, positioned on a goniometric table. A mica substrate ($n=1.58$ at 325 nm) with a dense needle area was positioned parallel to the planar surface of the half-sphere with the help of an immersion oil. The organic nanofibers were on the distant mica side with respect to the half-sphere. This is called in the following a two-phase (mica, air) TIR configuration.

Note that we take advantage of two specific properties of the nanofiber samples. Firstly, owing to their special growth mechanism, all the nanofibers are oriented strictly parallel to each other [Figs. 4(a) and 4(b)]. This allowed us to perform measurements with areas of densely packed nanofibers instead of trying to perform the measurement with a single nanofiber. Secondly, the height distribution function of the nanofibers for given growth conditions is very narrow, i.e., they all have roughly the same height [Fig. 4(b)]. This is important for a quantitative comparison between experiment and theory; see below.

The linearly polarized (extinction ratio 500:1) UV (325 nm) beam of a He–Cd laser was directed normally to the half-sphere convex surface, aiming at the center of the planar surface of the half-sphere (Fig. 5). We define TM- or TE-polarized incident light with the help of polarizers and a half-wave plate. The extinction ratio after the polarizers was 10^5. The fluorescence emitted from the organic nanofibers in the wavelength region around 430 nm was collected with a photomultiplier behind a bandpass filter while rotating the mica sample with the half-sphere over an angle of 2π in the mica surface plane. The rotation was performed in the *XY* plane, as according to Fig. 1. The axis of rotation was perpendicular to the mica surface and positioned in the center of the planar surface of the half-sphere. The UV beam was collimated before en-

tering the half-sphere, which resulted in a beam divergence of less than 0.7 deg at the surface plane. The size of the laser beam spot on the mica surface was ~300 μm in diameter.

RESULTS

During sample rotation we observed fluorescence maxima corresponding to a superposition of the EW's electric vector with the molecular transition dipole moments. We performed a series of measurements for both the TE and the TM cases with the same beam intensity (500 mW/cm^2) for different incident angles in the range below and above the critical angle. Typical experimental curves for two measurements above the critical angles are presented in Fig. 6.

The main source for the scatter in signal intensity is the nonhomogeneity of the nanofiber sample.

As seen in both cases a pronounced sinusoidal behavior is observed and the curves are shifted by $\pi/2$ with respect to each other. This is a strong qualitative proof of the elliptical character of the EW. For each measurement we fitted a sinus square function to the data and took the amplitude as a quantity proportional to the appropriate mean-square value of the electric vector component. This refers to the components that are nearly parallel to the molecular axis during rotation, i.e., E_x and E_y. The E_z component was taken as a pedestal in the TM case after subtracting the background level. Before fitting we took into account the angle of 5 deg of the molecular axis with respect to the surface plan[7] and projected it on the direction of the X and Z axes.

In the case of TM measurements the sinusoidal signal is due to the x component of the electric vector of the EW. The flat pedestal is a constant contribution due to the z component. The ratio of these two components is presented in Fig. 7 together with results from the two-phase TIR calculations.[4] We emphasize very good quantitative agreement of experimental and theoretical curves after multiplying the theoretical curves by a factor of 5.

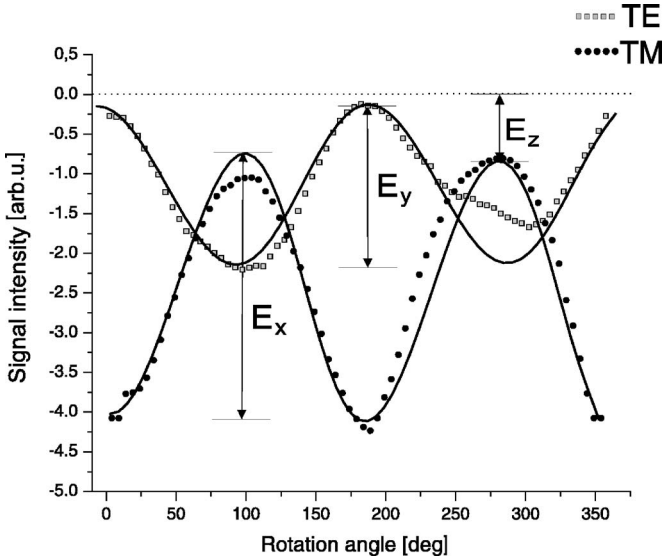

Fig. 6. Typical experimental intensity profiles for TM and TE polarizations in the two-phase configuration as a function of the angle of rotation. The fitted curve is a $\sin^2(\alpha)$.

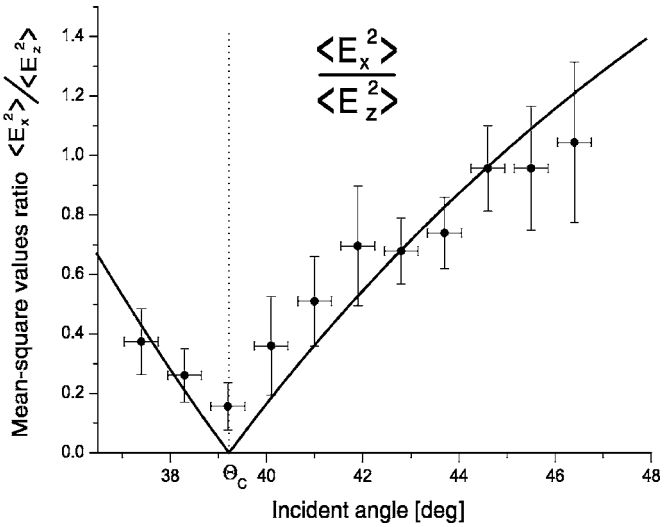

Fig. 7. Calculated and experimental ratio of mean-square values of electric vectors TE and TM in two-phase configuration as a function of the angle of incidence. Mica, air: $n_1=1.58$ and $n_2=1$.

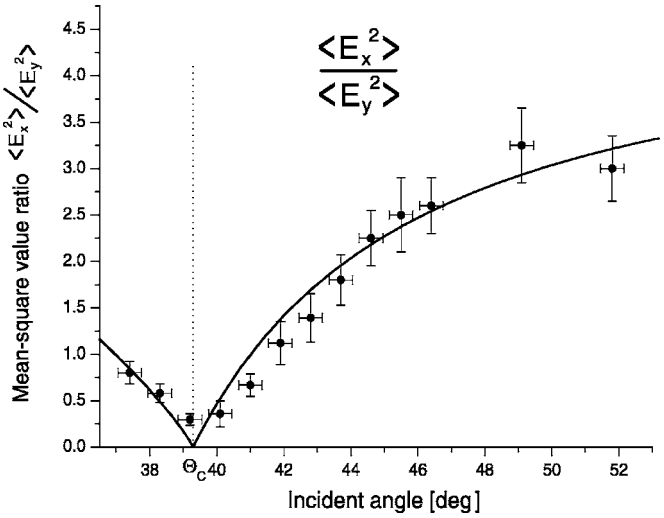

Fig. 8. Calculated and measured mean-square electric field x and y component ratio for the two-phase configuration as a function of the angle of incidence for $n_1=1.58$ and $n_2=1$..

In the two-phase TIR configuration we also made a series of measurements for TE and TM polarizations one by one with equal beam intensities, providing us with a more-direct way of determining the ratio of the field components. This method enabled us to suppress possible systematic errors due to a bleaching of the nanofibers, which occurred after long illumination.

The ratios of fluorescence intensities for TM and TE polarizations as a function of angle of incidence can be compared with those obtained from solving the Fresnel equations.[4] Both are presented in Fig. 8. Again, the agreement is very good after multiplying the experimental results with a factor of 6. We assign this factor to the strong dichroism of mica. It is different for the two experiments, since we have used two different slides of mica. We optically investigated the mica substrate without nanofibers and found the expected dichroism and no severe dependence of it on the angle of incidence in the range of 40 and

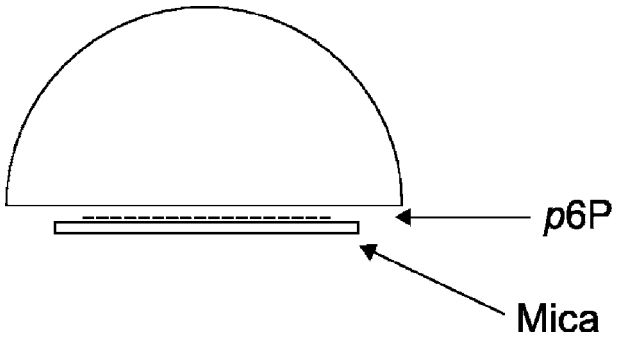

Fig. 9. Sketch of the three-phase TIR configuration.

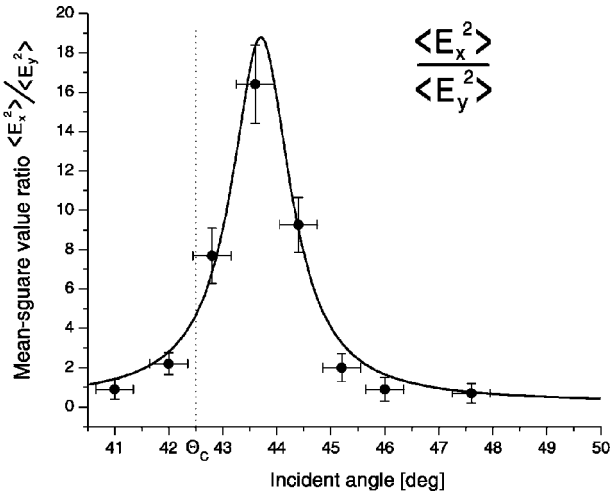

Fig. 10. Calculated and measured ratios of mean-square electric vector components for the three-phase configuration as a function of the angle of incidence. The indices of refraction are $n_1=1.48$, $n_2=1$, and $n_3=1.58$. The air-gap thickness is 200 nm, and the electric field in the gap was calculated to be as close as 50 nm (mean nanofiber thickness) to the mica surface.

50 deg. Owing to the experimentally given thickness of the sample used, the polarization direction has not been rotated by the mica plate. This test ensured that the prepared TM and TE polarizations in the incident wave were not changed after propagation through the mica substrate in the two-phase configuration.

Next we have performed a series of experiments in a three-phase configuration (quartz, air, mica; see Fig. 9). The nanofibers on the mica were oriented toward the half-sphere in that configuration, and there was a small (0.2 μm) air gap between the mica and the quartz half-sphere. Otherwise the experimental setup was not changed compared with the two-phase configuration.

A series of measurements for the TE and TM polarization cases was performed using equal light intensities. The ratios of $\langle E_x^2\rangle/\langle E_y^2\rangle$ are shown in Fig. 10 together with calculations for the three-phase TIR configuration.[4] The fitted curve height and position was very sensitive to the value of the distance of the calculated field from the mica surface. As seen from the height scan in Fig. 4 the maximum possible distance is about 80 nm. The fit of the theoretical curve to the experimental data resulted in a best-fit value of 50 nm, which is well within the limit given by the morphological measurements.

We emphasize very good agreement between experimental data and theoretical calculations. We would like to point out much smaller errors in the case of the ratio of E_x over E_y than in the case of the ratio of E_x over E_z ratio. In the first case we divided the amplitudes of two sinusoidal square functions of comparable magnitudes. In the second case we divided the amplitude of sinusoidal square function through the pedestal that was extracted with a relatively large error. In both series of measurements in the two-phase configuration, we did not reach zero for the critical angle. This discrepancy with the calculation might be due to the laser beam divergence and/or due to residual scattered light from the rough discontinuous organic film on the surface.

CONCLUSIONS

In this paper we presented a direct measurement of the ellipticity of the EW in the TM configuration by employing nanoscaled optical polarization probes, namely, organic nanofibers. In a two-phase configuration setup, the ellipticity of the EW as a function of the angle of incidence is proven directly by a measurement of the $\langle E_x^2\rangle/\langle E_z^2\rangle$ component ratio and indirectly by measurement of the $\langle E_x^2\rangle/\langle E_y^2\rangle$ ratio. In a three-phase configuration setup, owing to weaker signals, only the $\langle E_x^2\rangle/\langle E_y^2\rangle$ ratio could be measured, being also in very good agreement with the theoretical predictions. Overall the measurements confirm the theoretically predicted behavior of the polarization of the EW as a function of the angle of incidence for both TE and TM polarization cases.

ACKNOWLEDGMENTS

H.-G. Rubahn is grateful to the Danish research agencies Natural Science Research Council (21-03-0469) and Statens Teknisk-Videnskabelige Forskningsråd (26-04-0253) for supporting this work. J. Fiutowski received a partial grant from the Erasmus/Socrates program.

L. Józefowski is the corresponding author and can be reached via e-mail at ufjozefo@cyf-kr.edu.pl.

REFERENCES

1. J. A. Stratton, *Electromagnetic Theory* (McGraw-Hill, 1941).
2. S. Huard, *Polarization of Light* (Wiley & Sons, 1997).
3. F. de Fornel, *Evanescent Waves* (Springer, 2001).
4. W. Hansen, "Electric fields produced by the propagation of plane coherent electromagnetic radiation in a stratified medium," J. Opt. Soc. Am. **58**, 380–390 (1968).
5. T. Kawalec, M. J. Kasprowicz, L. Jozefowski, and T. Dohnalik, "Zeeman effect observed in the EW," Acta Phys. Pol. A **105**, 349–355 (2004).
6. F. Balzer and H.-G. Rubahn, "Dipole-assisted self-assembly of light-emitting p-nP needles on mica," Appl. Phys. Lett. **79**, 3860–3860 (2001).
7. H. Plank, R. Resel, S. Purger, J. Keckes, A. Thierry, B. Lotz, A. Andreev, N. S. Sariciftci, H. Sitter, "Heteroepitaxial growth of self-assemled highly ordered para-sexiphenyl films: a crystallographic study," Phys. Rev. B **64**, 235423 (2001).
8. F. Balzer and H.-G. Rubahn, "Growth control and optics of organic nanoaggregates," Adv. Funct. Mater. **15**, 17–24 (2005).